Electronic Supplementary Material (ESI) for Dalton Transactions

Photomagnetic Studies on Spin-Crossover Solid Solutions Containing Two Different Metal Complexes, $[Fe(1\text{-}bpp)_2]_x[M(terpy)_2]_{1-x}[BF_4]_2$ (M = Ru or Co)

Guillaume Chastanet[a], Clare A. Tovee[b], Geoffrey Hyett[b], Malcolm A. Halcrow[b] and Jean-François Létard[a,*]

[a]*CNRS, Université Bordeaux, ICMCB, Groupe des Sciences Moléculaires, 87 Av. Doc. A. Schweitzer, F-33608 Pessac, France. Email: letard@icmcb-bordeaux.cnrs.fr*

[b]*School of Chemistry, University of Leeds, Woodhouse Lane, Leeds LS2 9JT, UK. E-mail: m.a.halcrow@leeds.ac.uk*

Electronic Supplementary Information

Figure S1 Observed (black) and simulated (red) powder *X*-ray diffraction patterns for $[Fe(1\text{-}bpp)_2]_x[Ru(terpy)_2]_{1-x}[BF_4]_2$ (**1**-**6**).

Figure S2 Observed (black) and simulated (red) powder *X*-ray diffraction patterns for $[Fe(1\text{-}bpp)_2]_x[Co(terpy)_2]_{1-x}[BF_4]_2$ (**1** and **7**-**9**).

Table S1 Unit cell dimensions of $[Fe(1\text{-}bpp)_2]_x[Ru(terpy)_2]_{1-x}[BF_4]_2$ (**1**-**6**) from powder diffraction simulations.

Table S2 Unit cell dimensions of $[Fe(1\text{-}bpp)_2]_x[Co(terpy)_2]_{1-x}[BF_4]_2$ (**7**-**9**) from powder diffraction simulations.

Figure S3 Variation of the unit cell volume *V* with composition for $[Fe(1\text{-}bpp)_2]_x[M(terpy)_2]_{1-x}[BF_4]_2$.

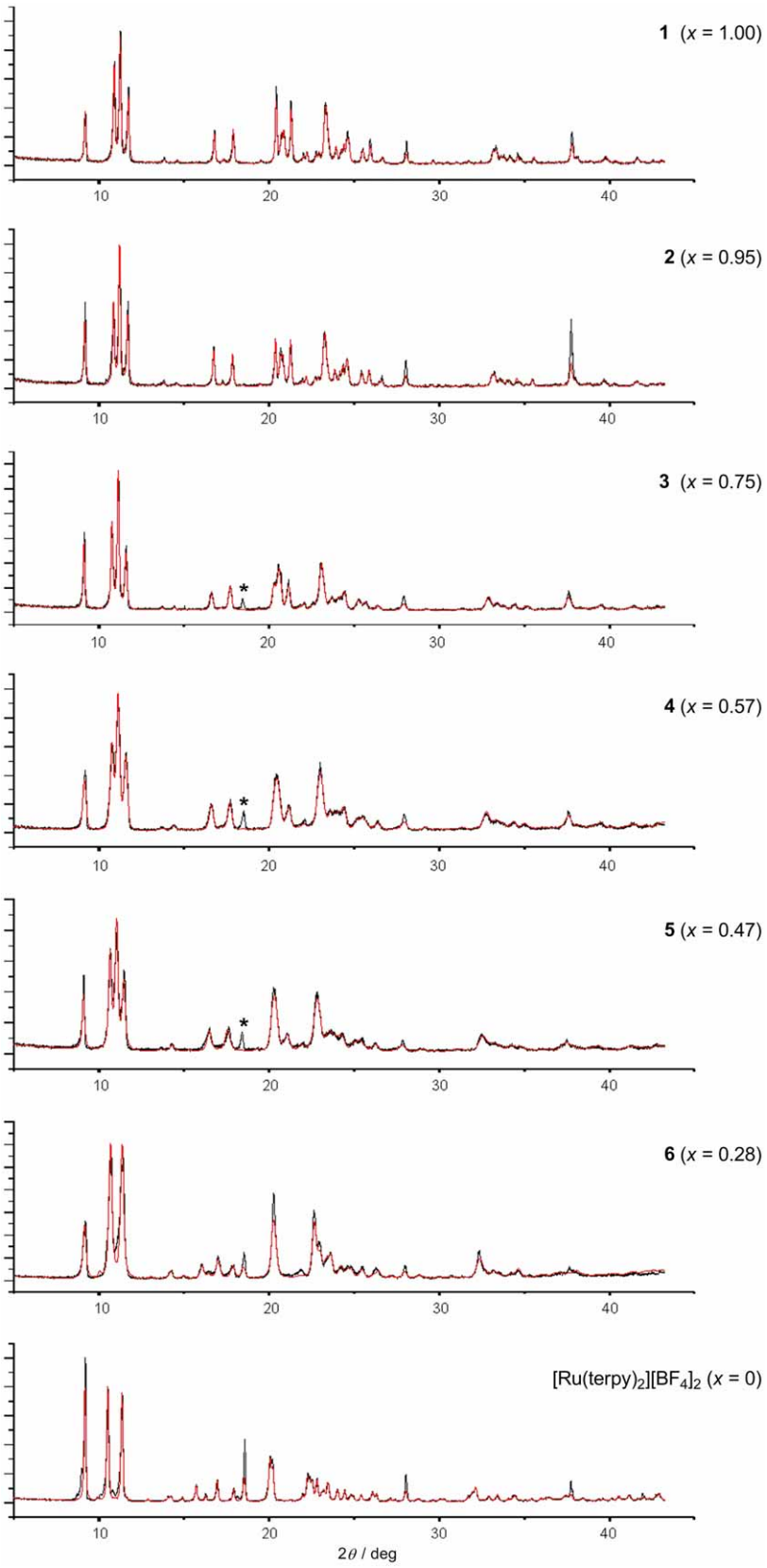

Fig. S1 Observed (black) and simulated (red) powder *X*-ray diffraction patterns for $[Fe(1\text{-bpp})_2]_x[Ru(terpy)_2]_{1-x}[BF_4]_2$ (**1**-**6**). The starred peak for $0.75 \geq x \geq 0.47$ indicates the presence of the *Cc* phase as a minority contaminent, in the $P2_1$ phase adopted by the bulk of these materials.

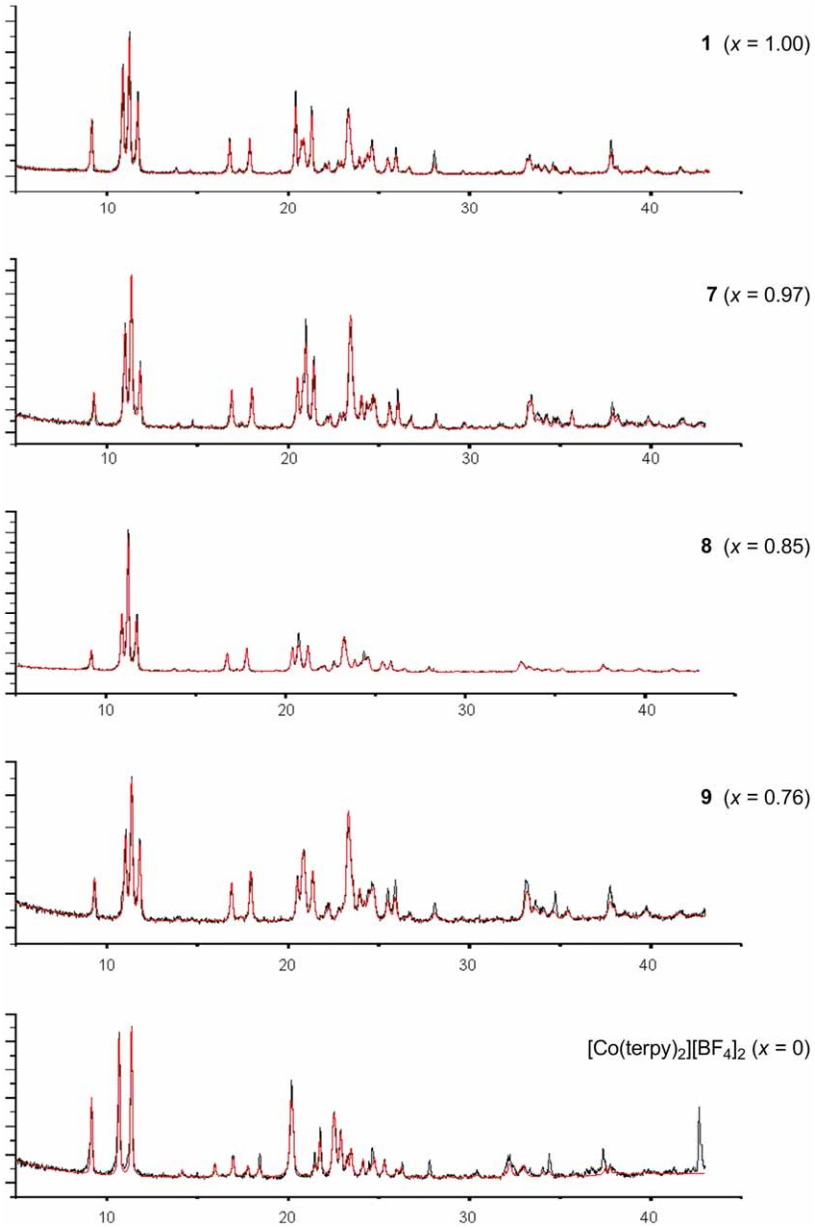

Fig. S2 Observed (black) and simulated (red) powder *X*-ray diffraction patterns for $[Fe(1\text{-bpp})_2]_x[Co(terpy)_2]_{1-x}[BF_4]_2$ (**1** and **7-9**). The results of the simulations are given in Table S1.

Table S1 Unit cell dimensions of $[Fe(1\text{-bpp})_2]_x[Ru(terpy)_2]_{1-x}[BF_4]_2$ (**2-6**) and the relevant precursor compounds $[Fe(1\text{-bpp})_2][BF_4]_2$ (x = 1.00, **1**) and $[Ru(terpy)_2][BF_4]_2$ (x = 0), from powder diffraction simulations (Fig. S1). The unit cell volumes calculated from these parameters are listed in Table 1 of the main paper.

	x	Space group used in simulation	a, Å	b, Å	c, Å	β, °	V, Å^3
1	1.00	$P2_1$	8.49	8.51	19.05	95.6	1369.2
2	0.95	$P2_1$	8.51	8.53	19.07	95.6	1376.8
3	0.75	$P2_1$[a]	8.58	8.59	19.14	95.5	1404.6
4	0.57	$P2_1$[a]	8.62	8.63	19.14	95.5	1416.6
5	0.47	$P2_1$[a]	8.67	8.66	19.16	95.4	1432.0
6	0.28	*Cc*	12.41	12.31	19.17	96.6	2910.3
	0	*Cc*	12.61	12.39	19.18	98.0	2965.7

[a]These materials are predominantly in the $P2_1$ space group, but also appear to contain a minor fraction of the *Cc* phase (Figs. S1 and S2). This contaminent could not be incorporated into the simulations.

Table S2 Unit cell dimensions of $[Fe(1\text{-bpp})_2]_x[Co(terpy)_2]_{1-x}[BF_4]_2$ (**7-9**) and the relevant precursor compounds $[Fe(1\text{-bpp})_2][BF_4]_2$ (x = 1.00, **1**) and $[Co(terpy)_2][BF_4]_2$ (x = 0), from powder diffraction simulations (Fig. S2). The unit cell volumes calculated from these parameters are listed in Table 1 of the main paper.

	x	Space group used in simulation	a, Å	b, Å	c, Å	β, °	V, Å^3
1	1.00	$P2_1$	8.49	8.51	19.05	95.6	1369.2
7	0.95	$P2_1$	8.50	8.52	19.06	95.6	1372.9
8	0.85	$P2_1$	8.53	8.55	19.14	95.5	1390.6
9	0.76	$P2_1$	8.57	8.57	19.17	95.4	1401.8
	0	*Cc*	12.57	12.42	19.37	96.7	3000.7

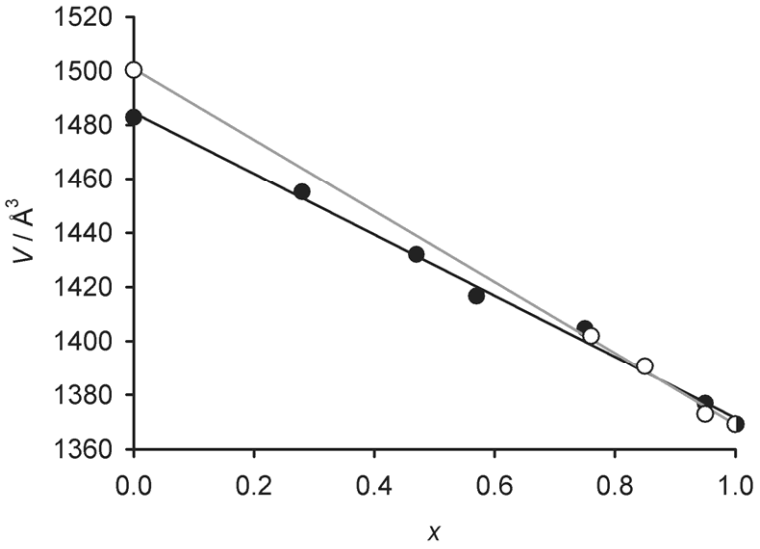

Figure S3 Variation of the unit cell volume V with composition for $[Fe(1\text{-bpp})_2]_x[M(terpy)_2]_{1-x}[BF_4]_2$ for M = Ru (**1**-**6**; ●) and M = Co (**1** and **7**-**9**; ○). Lines of best fit are drawn through both sets of data. Volumes for the materials in the *Cc* phase are normalised to $Z = 2$.